INTERNATIONAL JOURNAL OF INTEGRATED ENGINEERING
ISSN: 2229-838X e-ISSN: 2600-7916

IJIE

Vol. 16 No. 6 (2024) 254-264
https://publisher.uthm.edu.my/ojs/index.php/ijie

Investigating the Effect of Porosity and Pore Shape on Porous Polymer Structure Under Axial Compression and Buckling Behaviour

Ab Aziz bin Mohd Yusof[1]*

[1] *School of Mechanical Engineering, College of Engineering, Universiti Teknologi MARA, UiTM, Johor Branch., Masai, Johor, MALAYSIA*

*Corresponding Author: abaziz86@uitm.edu.my
DOI: https://doi.org/10.30880/ijie.2024.16.06.025

Article Info

Received: 16 May 2024
Accepted: 24 November 2024
Available online: 29 December 2024

Keywords

Porous polymer, axial compression, buckling, porosity, pore shape

Abstract

The strength and durability of porous polymer structures under compression and buckling remain a significant challenge in engineering. Despite extensive research on the porous structure related to polymers, the failure mechanics and the characteristics of the porous polymer structure were found to be limited. There is a need to investigate the underlying mechanisms of porous polymers to develop accurate strategies to improve their mechanical properties and stability. Therefore, the study was carried out to investigate the effect of the porosity and pore shape under axial compression and buckling. The porous polymer's square and circular pore shape was fabricated using 3D printing for five structure porosities: 30%, 40%, 50%, 60%, and 70%. The printed samples were placed on the tensile testing machine and compressed axially at 3 mm/min speed. Higher porosity led to significant stress reduction, with a linear decrease in maximum compression force correlating with porosity, and circular pores exhibited better performance. The Pearson correlation highlighted a consistent, predictable inverse relationship between porosity and compression force with the coefficient of square pore at r = -0.981 and for circular pore at r = -0.986. In conclusion, the study revealed the complex mechanical behaviour of a porous polymer under compression.

1. Introduction

Porous polymers have a wide range of applications due to their unique structure and properties. The presence of pores within the polymer matrix makes them useful in various fields. It is used in electronic devices as sensors, energy storage, biomedical applications such as scaffolds, separation, and purification such as filters [1, 2]. The mechanical properties of porous polymers can be tailored during the design and synthesis process to meet the specific requirements of each application. Factors such as pore size, pore distribution, and overall material composition can be adjusted to optimise mechanical strength and flexibility. Besides, there is a need to understand the failure mechanisms of porous polymer structures, which aids in evaluating their durability and long-term performance, including biomedical, material properties enhancement, and energy absorption structure [3-5]. This aspect is particularly important in industries where these materials are used for load-bearing structures or when subjected to mechanical stresses. Therefore, the mentioned work suggested the opportunity to explore further and understand the relationship between porous structure design parameters such as porosity and pore shape toward their mechanical performance to develop innovative, application-specific porous structures that meet the diverse demands of various industries.

This is an open access article under the CC BY-NC-SA 4.0 license.

The porous structure has a significant impact on engineering applications. In recent years, there has been an increase in the demand for porous structures made from polymer material like polylactic acid (PLA), acrylonitrile butadiene styrene (ABS), polystyrene (PS) polymers, polyurethane (PU) and polyvinyl chloride (PVC) [6, 7]. These structures have advantages such as permeability to absorb or desorb the liquid. In addition, the porous structure also has advantages such as high flexibility, high energy absorption capability, a better insulator for heating electrical charges, and a good damper for mechanical vibration.

Porous polymers can be used as scaffolds for tissue engineering applications. These scaffolds provide a three-dimensional structure that supports cell growth and tissue formation. The ability to withstand compression forces is crucial for applications where the scaffold needs to mimic the mechanical properties of natural tissues [7, 8]. In medical applications, porous polymers are used as bone scaffolds to provide mechanical support to the regenerating tissue during the healing process. This particular structure is important in load-bearing areas where the scaffold helps withstand mechanical forces and maintain stability while new bone forms. The study done by S. A. Park et al. (2018) demonstrates the capability of the bone scaffold to promote bone regeneration for defect healing in the bone, as shown in Figure 1 (b) [9]. The pore structure supports the defect area by stabilising the area from the external load while facilitating bone generation.

3D printing also proves its capability to fabricate porous structures using polymer material to the micro scales. The product size could be as big as the bulk scale or as tiny as the micro-scale, for example, microelectromechanical systems (MEMS) [10]. Y. Xue et al. (2020) reported that integrating electrospray and digital light processes can produce a 3D porous microstructure, as shown in Figure 1(a). The product can be applied as a microelectromechanical MEMS system for the power-free pressure sensor. The porous polymers are integrated into MEMS devices to act as structural elements for electrical properties or to provide mechanical flexibility while fulfilling the device's function [11]. Besides that, the high sensitivity of capacitive pressure sensors with better durability was developed using a porous polymer structure for advanced device application [10].

Compression and buckling are two types of force that constantly act on the loaded structure. The combination of these forces causes complex multiaxial load conditions. In bone scaffold applications, the ability to withstand compression forces is crucial for applications where the scaffold needs to mimic the mechanical properties of natural tissues. MEMS devices especially use cantilever beams exposed to bending force that compromises tension and compression forces during operation. Porous polymers can be integrated into MEMS devices to act as structural elements or to provide mechanical flexibility while maintaining the overall integrity of the device. The cantilever structure of the MEMs is made from porous polymer [12]. Meanwhile, in automotive applications, porous polymer was used in vibration applications [13].

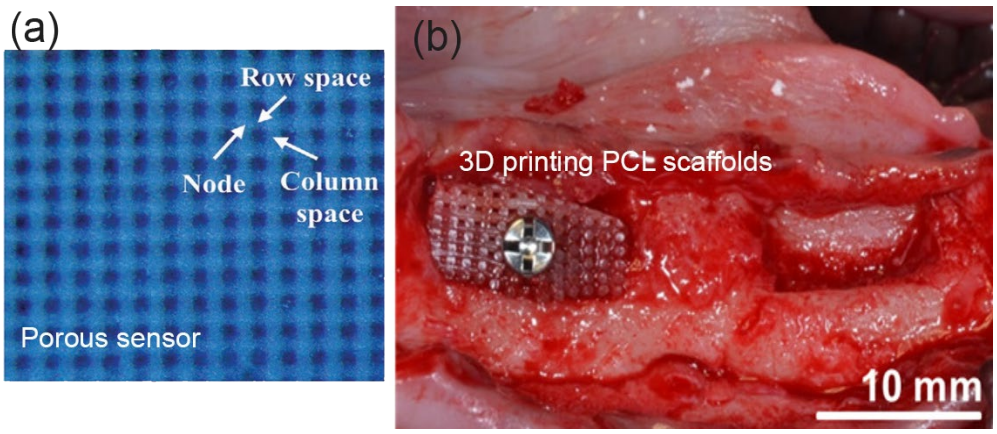

Fig. 1 *Example of porous polymer application adapted from [10] and [9]*

Based on the mentioned issues of porous polymer and loading condition, the study was carried out to investigate the effect of porosity and pore shape on the mechanical properties of the polymer under compression and buckling. Despite many studies done on the compression of the porous polymer, to the best of the author's knowledge, the study of the study on mechanical properties of the porous polymer under compression, which leads to buckling, is limited even though there are many applications of the porous polymer involve the combination of compression and buckling. It is important to address the effect of the porosity and pore size related to the porous polymer on the structural characteristics; thus, the strength and mechanical characteristics of the structure can be manipulated to fulfil its function. The study focused on the additive manufacturing process of 3D printing to fabricate the sample. PLA material was used as the investigated material since it is readily available in the market and is used in many engineering applications.

Int. Journal of Integrated Engineering Vol. 16 No. 6 (2024) p. 254-264

2. Material and Method

2.1 Parameters Study

Figure 2 shows the model of the sample used in the study. For simplification, the model was managed as a homogeneous material where the young modulus of the polymer material, *E*, was assumed to be the same for the whole structure. According to Euler's formula, the critical buckling load of the compressed porous polymer directly proportional to the material's modulus of elasticity and moment of inertia of the cross-sectional area, *I,* which is both were adjusted according to structure porosity as shown in Figure 2 [14]. Meanwhile, the critical buckling load was inversely proportional to the column's effective length factor, *K,* which is then *K* dependent on the end condition and the effective length of column *L*.

The simplified approach of the critical buckling load for the porous polymer in cylindrical shape under axial compression, as in Figure 2, can be represented in Equation (1) [15].

$$P_{cr} = \frac{\pi^2 EI}{(KL)^2} \tag{1}$$

It is important to note that this is a simplified equation, and adjusting the modulus of elasticity, *E,* and moment of inertia (I) for porosity might be more complex and dependent on the specific material properties. Generally, the second moment of a porous structure could be obtained in a non-uniform shape, in which the value of *A* depends on the porosity of the tested sample.

$$I_{xx} = \int_A y^2 \, dA \tag{2}$$

A is the cross-sectional area, and *y* is the perpendicular distance from the axis to the differential area element *dA*. However, since porosity was manipulated besides the pore shape to investigate the mechanical characteristics of the porous polymer, the porosity factor was then included in Equation (2) to become Equation (3).

$$P_{cr} = \frac{\pi^2 EI}{(KL)^2} (1 - \emptyset) \tag{2}$$

$\emptyset$ is the porosity factor (ranging from 0 to 1, where 0 is dense material and one is fully porous). In this study five numbers of porosity were selected in the study, the expected porosity factor are 0.3,0.4,0.5,0.6 and 0.7. From the Equation, it was expected that increasing the porosity would cause the critical load to be decreased, which can be represented by the stress-strain graph and maximum compression force of each sample.

In this study, porous polymer structures were designed by manipulating the pore configuration and structure. The structures were designed based on two strategies to form different morphology: Percentage of porosity and shape of the pore. Two basic pore shapes, square and circular pore, were considered to compare the smooth circular shape and conner rectangular of square pore.

The pore was aligned in a specific orientation, as shown in Figure 2 and interconnected by forming a network that influenced its mechanical behaviours. The pore size was then manipulated to obtain different porosities between 30 and 70 per cent based on the porosity formula, in which the void volume was divided by the total volume of the samples. The dimension of the square pore length varied from 0.77 mm to 1.29 mm, and the diameter of the circular pore varied from 0.86mm to 1.49 mm. There are about ten different sizes of squares to circular to fabricate as porous polymer structures based on this setting. The porous polymer model was designed using SolidWorks software. The important aspects of the intended use, size, complexity, and material requirements were considered to smooth the design process. The cross-section area to calculate stress acted on the sample during the test was taken at the middle of the structure and measured based on the SolidWorks model. According to the study by B. Dorweiler et al. (2021), comparing the dimensions between the designed model and printed parts is less than 1mm or 5%, which accurately demonstrates the printed parts [16].

The structure was designed as a cylindrical shape with a 10 mm diameter and 30 mm height. The diameter-to-height ratio was 33 per cent, which was lower than 40 per cent for the standard compression test to consider the buckling effect during the compression test [17]. A total of 10 porous structure models with different pore shapes and porosity were saved in Standard Tessellation Language, STL, which is compatible with 3D printers.

The next step was to fabricate the samples. 3D printing technology of Fused Deposition Modeling (FDM) was used to form the porous polymer structure [18]. This process was preferred as it was highly customisable and could create complex geometries. Besides that, additive Manufacturing or 3D Printing was known to fabricate electronic parts, MEMS devices, and bone scaffolds. The study used polylactic acid, PLA, as the main material to fabricate the porous structure. The advantages of this thermoplastic material are a high-modulus polymer, easy processing, and good stiffness.

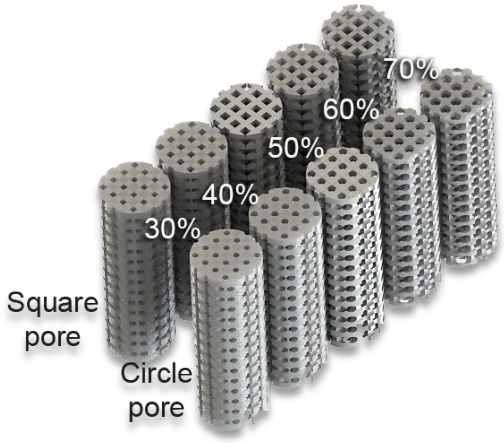

Fig. 2 Model of square and circular pore sample used in the study

Table 1 *3D printing parameters for the porous polymer sample*

Printing parameter	Detail
Nozzle temperature	220 ºC
Bed temparature	60 ºC
Printing speed	80 mm/s
Layer height	0.2mm
Infill density	100%

The STL model of the porous sample was then converted into printable layers based on the G-code using Creality Slicer 4.8.2 software provided by the manufacturer; the printing setting was provided as in Table 1. 0.20mm layer height was set to match the layer height of the printer. The printer nozzle was heated to 200 degrees Celcius. In comparison, the printing bed was set at 60 degrees Celsius to ensure the filament melted properly and stuck on the printing platform for the whole printing process. Besides that, with the proper heating, layer adhesion issues could be eliminated. The finished product of porous polymer made from PLA was inspected to ensure its smooth surface; both ends were flat, and the pore axis was parallel.

2.2 Experimental Setup

The printed samples were subjected to compressive forces to evaluate their behaviour under compression, typically by applying a uniaxial force. This assesses the maximum compressive stress the material can withstand before failure and examines the deformation characteristics, such as force and displacement. Additionally, buckling, a specific failure mode where structures suddenly deflect laterally due to instability under compression, is particularly significant in porous components. The study focused on understanding the relationship between compression and buckling. Thus, compression testing provides crucial data on a material's capacity to endure compressive forces, while buckling is essential for ensuring structural stability under compression.

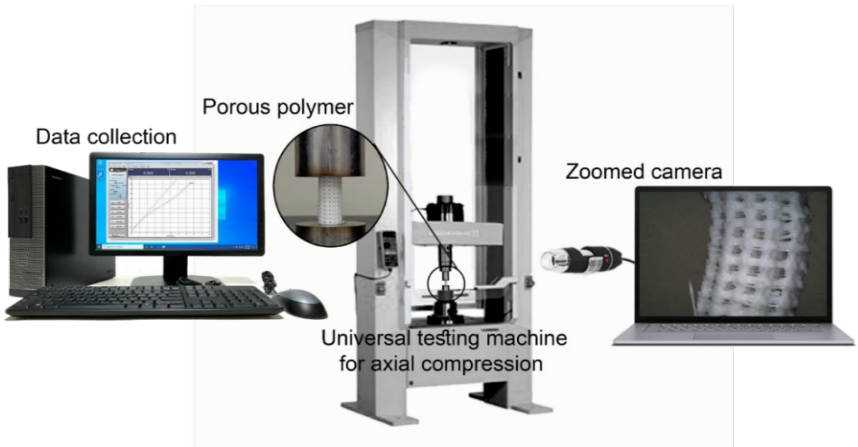

Fig. 3 *Axial compression test setup*

Int. Journal of Integrated Engineering Vol. 16 No. 6 (2024) p. 254-264

The axial compression test was carried out using a tensile testing machine (Shimadzu, AGX-V Series, North America), as in Figure 3. The porous polymer structure was placed by the two hardened jigs with fixtured slots and compressed until the fracture point was set at 11mm displacement or 37 per cent of strain. The value was decided based on this experimental data as the sample fully buckled under the compression. Both specimens (square and circular pore) were tested during the study, as shown in Figures 4 a) and 4 b). Cross-head speed was moved at 3 mm/min to compress the sample axially [14]. At the same time, structural response under the applied load was recorded using a Digital microscope 1000x magnification camera (Model X4) placed in front of the sample as shown in Figure 3. At least five specimens were tested for each porosity to make 50 total tested samples, and data was recorded.

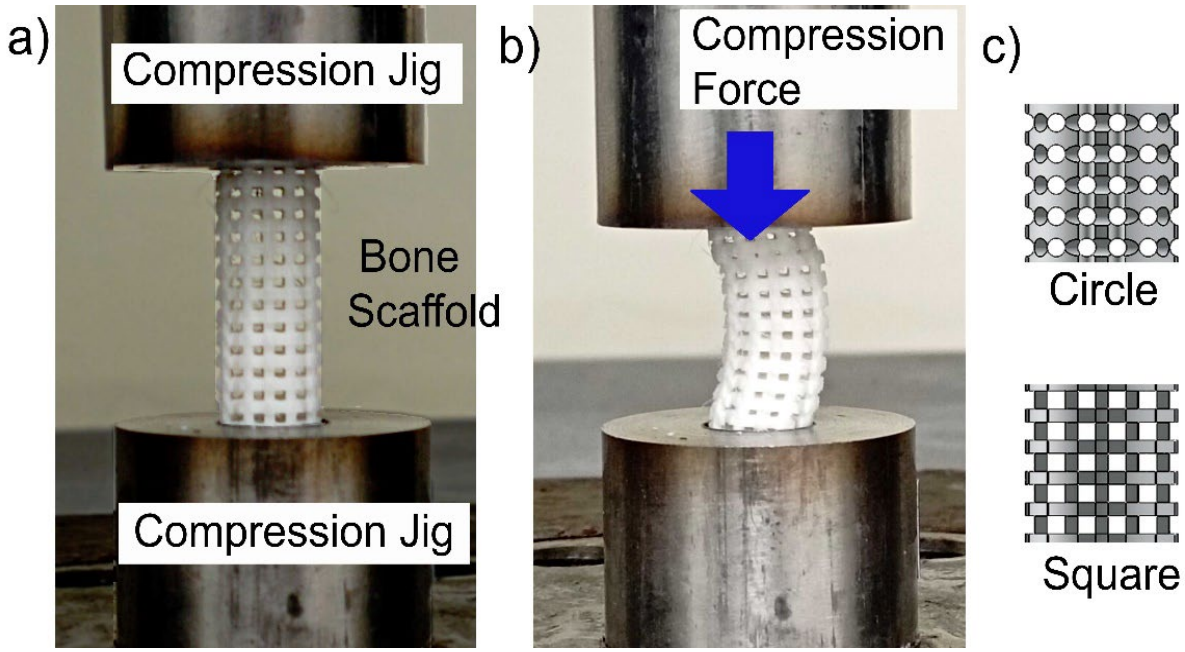

Fig. 4 *(a) Initial sample condition placed on the jig; (b) Sample under the compression; (c) Pore structure*

2.3 Statistical Analysis

All the collected data went through data post-processing using statistical procedures to derive meaningful insights into the collected data. In the first step, the data was expressed as mean and standard deviation to obtain the general pattern of the data, which helps in understanding the data's central tendency (mean) and variability (standard deviation). The t-test and Pearson correlation test using IBM SPSS Statistics 23 (IBM Corp, USA) [19]. A t-test was used to test the means of the experimental value and whether there was a difference between the response of porous polymer due to porosity and pore shape. Besides that, the correlation between each factor was tested using the Person correlation test. The priory alpha of $p < 0.05$ was set to the data represented statically significant level of 5%.

3. Result

3.1 Axial Compression and Buckling Characterization

As the percentage of the porosity varied from 30 per cent to 70 per cent, the maximum compression force was reduced linearly for both square and circular pores, as shown in Figure 5. The graphs show that the porosity of a material influences its maximum compression force-bearing capacity. Higher porosity generally leads to lower compression strength. For 30 per cent of porosity, the circular pore has a higher maximum compression force than a square pore. The difference in maximum compression force was then reduced as porosity increased, intersecting at 50 per cent of porosity. For the higher tested porosity, 50 per cent, 60 per cent and 70 per cent, the maximum compression force experienced by the circular pore was lower than the square pore.

Generally, circular pores form a more robust porous polymer structure with a gradient of -39.91N/percentage of the porosity. Meanwhile, the maximum compression force gradient versus the percentage of porosity for the square pore was -29.35N/percentage of porosity. The graphs exhibit linear relationships, implying a consistent change in maximum compression force with changes in porosity. The rate of change refers to the slope of the line.

It provides quantitative information about the sensitivity of the material to changes in porosity, in which circular pores acted by adding more than 10N per percentage of porosity to the porous polymer structure.

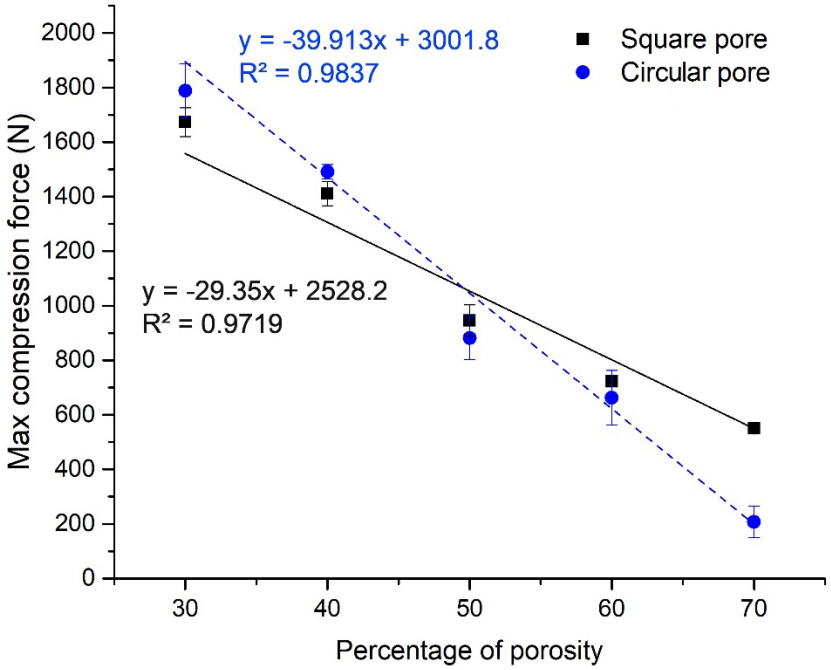

Fig. 5 *Effect of the percentage porosity to maximum compression force*

The porous polymer compressed under axial compression behaves mechanically, as shown in Figure 6. 30 to 70 per cent porosity for both circular and square pore shapes were extracted for comparison. In the first compression stage, a porous structure subjected to axial compression undergoes elastic deformation for the tested samples. At this stage, the structure deforms reversibly and will return to its original shape once the compressive load is removed. Linear behavior is known as the modulus of elasticity, defined as the ratio of stress to strain within the elastic range of a material. Young's modulus recorded for the circular pore are 6.68MPa, 6.36MPa, 4.08MPa, 3.69MPa, and 1.57MPa respectively, for 30%, 40%, 50%, 60%, and 70% of porosity. For Square pores, the Young's modulus recorded are 6.51MPa, 6.78MPa, 4.61MPa, 4.26MPa, and 3.15MPa for 30%, 40%, 50%, 60%, and 70% of porosity. Generally, the young's modulus value reduced the exponentially as the porosity increased

As the stress increases beyond the elastic threshold, the material yields, and plastic deformation begins. This stage was associated with permanent deformation even if the load was removed. The curve rises steeply, indicating a transition to a densified state where the material behaves more like a dense. Indicates the structure and material's ability to absorb energy through plastic deformation. As the structure passed the maximum stress, it started to experience buckling, which led to the bending of the structure. This deformation was primarily due to the bending and stretching of the structural struts. As the axial compression continued to apply by lowering the cross-head further, the magnitude of stress experienced on the porous structure dropped suddenly from maximum to lower stress value, which on average by 55±15 per cent stress drop for the circular pore and 56±24 per cent stress drop for the square pore.

Figure 7 shows the porous structure response under compression for 40 per cent and 60 per cent porosity samples. These two porosities were selected to represent the high and low porosity groups. In this study, 30%, 40% and 50% were categorized in the low porosity group, and 60% and 70% were categorized in the high porosity group. The first two images of the porous structure in Figures 7 (a) and 7(b) show that the structure experienced elastic deformation under the compression load. A slight downward movement happened on the structure compared to the initial image. This elastic condition can be related to Figure 5. This elastic deformation of the tested sample happens at a strain less than 5 per cent.

Besides, as shown by the third image in Figure 7, the porous structure experienced maximum stress, leading to buckling as the structure lost structural stability and began to bend. As the buckling happened, stress softened, and the stress experienced decreased under constant strain. In the context of compression testing, primary stress softening is the initial reduction in stress observed as the material undergoes compression. The phenomenon is typical behavior in specific polymers and elastomers. Further increasing the compression load causes the secondary stress softening to happen. At this point, the strut looks to collapse beyond the critical points where the material's strength decreases more rapidly. Besides that, all the tested samples slipped to the side, and the

Int. Journal of Integrated Engineering Vol. 16 No. 6 (2024) p. 254-264

horizontal struts touched each other. The subsequent phase of stress softening is beyond the primary softening. This secondary softening occurred under prolonged compression, which introduced additional strain.

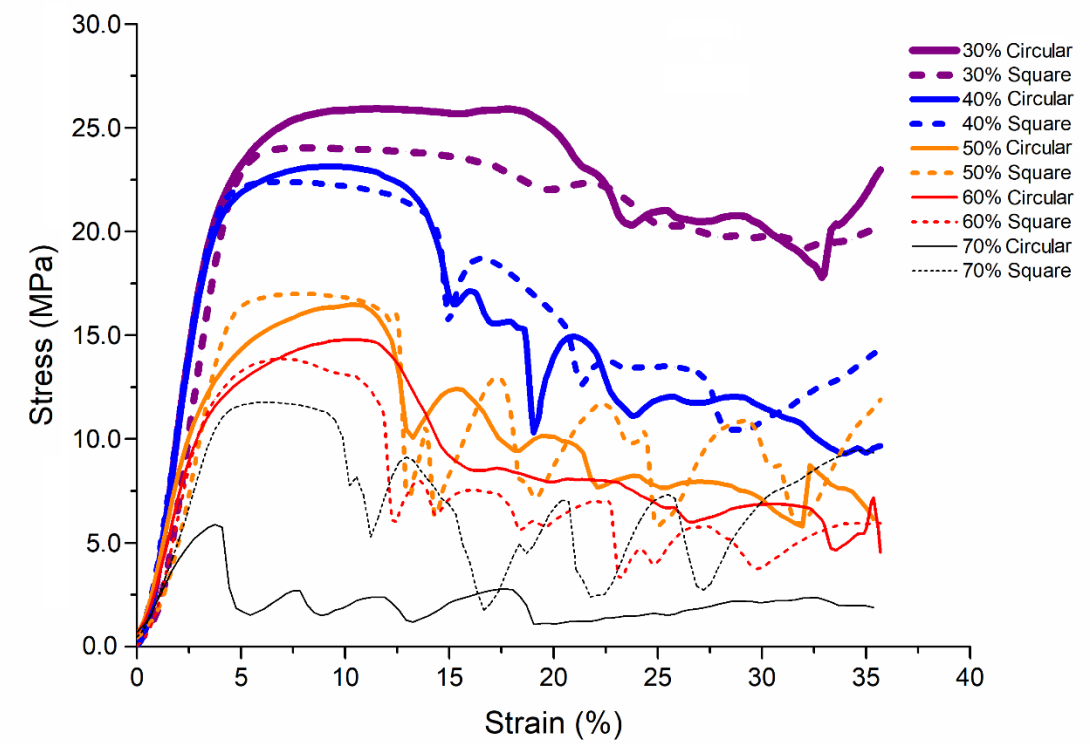

Fig. 6 *Stress-strain curve of circular and square pore*

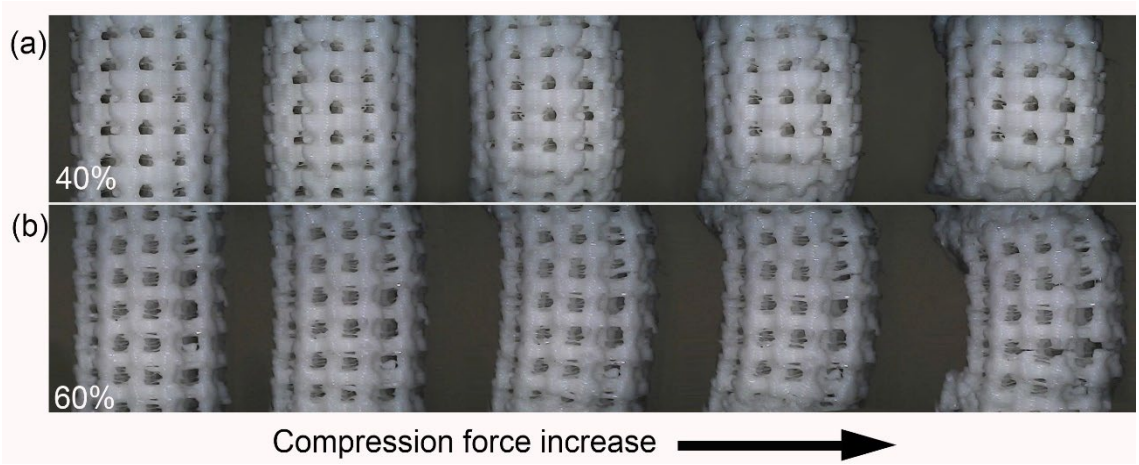

Fig. 7 *Struct deformation under the compression of 40 per cent and 60 per cent of circular pore*

Under buckling conditions, the porous structure experiences tension and compression on both sample sides. For the 40 per cent of porosity, the structure could hold both experienced stresses without fracture or crack. However, for the higher porosity structure, most of the sample cannot withstand the tension stress and cause a crack in the buckling location, contributing to the fracture of the structure. Besides that, The bending condition of the structure can induce additional stresses, especially in regions already experiencing high stress due to buckling. This can lead to the initiation and propagation of cracks.

The collapse sample of the porous polymer and the untested sample are shown in Figure 8. A considerable difference happened to the collapse sample as the axial compressive load was applied. More extensive deformation happens near both ends of the porous structure, where the buckle occurs in the middle. During the axial compression, both sides of the strut begin to collapse as it cannot hold the force increment. As the force increased, all the affected struts collapsed, eliminating the pore.

When comparing square and circular pores, square pores collapsed more as the curved wall strengthened the porous strut of the circular pore, as shown in Figure 9. Figure 9 (a) shows that square pores have sharp corners acting as stress concentrators. The stress is not uniformly distributed, leading to higher corner concentrations.

This makes square pores prone to crack initiation and fracture higher. Under the compression load, circular pores distribute stress more evenly around their perimeter, as shown in Figure 9 (b). This leads to lower stress concentrations at any single point than square pores.

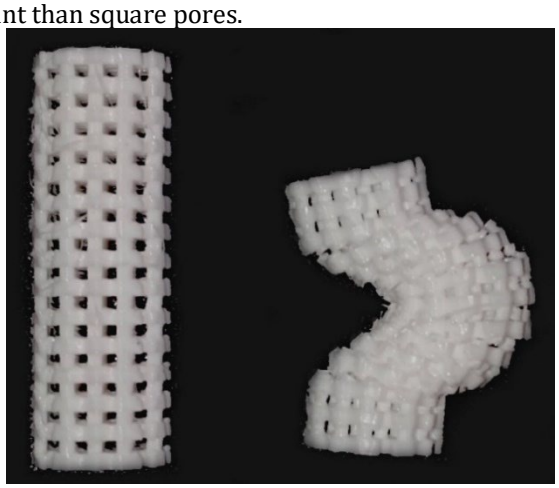

Fig. 8 *Comparison between samples of porous polymer before and after test*

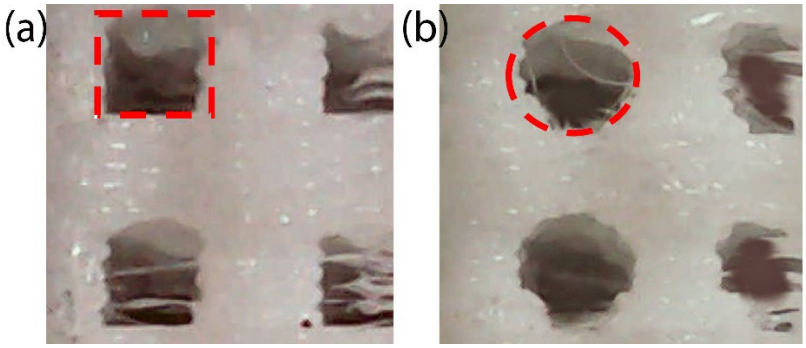

Fig. 9 *Comparison between pore sample (a) Square pore; (b) Circular pore*

3.2 Statistical Analysis from Experimental Data

An independent sample test was conducted on the collected data to compare the maximum compression force for square and circular pores. There were no significant differences (t(28) = 0.255 p= 0.80 in the mean score for square pore (m = 1054.67 SD = 436.788) was higher compared to circular pore (M = 1006.133 SD = 592.70) magnitude of the different in the mean (mean different = 48.53, 95% Cl -340.87: 437.94 to was no significant.) According to the Pearson correlation test, porosity had a strong negative correlation to the maximum compression force with the Pearson correlation coefficient of square pore is r = -0.981 and for circular pore r = -0.986, which both indicate a robust inverse relationship between porosity and maximum compression force. The statistical result indicates an almost perfect linear relationship between the porosity and maximum compression force. The linear relationship indicates that changes in one variable (porosity) are highly predictive of changes in another variable (maximum compression force) and vice versa.

4. Discussion

4.1 Mechanical Characteristics of the Porous Polymer Under Axial Compression

The buckling and collapsing of pores happened as the compression stress increased, and individual pores within the structure started to buckle or collapse with the loaded load. The porous structure was compressed in the early compression stages, reducing the length. The situation can result in increased material density as the length is reduced. The structure behaves to have good energy absorption characteristics. They may deform extensively during compression, dissipating energy and providing impact resistance. Beyond the elastic region, the porous structure undergoes plastic deformation. Plastic deformation is irreversible, and the structure may experience permanent changes in shape. In this case, plastic deformation was identified at the lower and upper part of the sample, where the strut experiences progressive collapse and the failure of individual components. Further strength reduction was induced by localization stress at certain regions within the structure, which can lead to stress concentrations in other areas, accelerating the failure process. The buckling of the structure causes global

Int. Journal of Integrated Engineering Vol. 16 No. 6 (2024) p. 254-264

instability as the entire structure experiences buckling or instability, which could lead to sudden and catastrophic failure.

As porosity increases, for example, in this study, the porosity varied from 30% to 70%, the material's Young's modulus decreases significantly, reflecting a substantial reduction in stiffness and load-bearing capacity. This aspect related to the microstructure of the porous polymer, as the material composition used was the same. The mechanical properties of the could be explained based on the power law relationship model $E_p = E_0 (1-P)^n$, Where E_p is the Young's modulus of the porous material, E_0 is the Young's modulus of the non-porous material, p is the microstructural parameters, and n is an empirical constant that depends on the material and its microstructure [20]. According to the formula and reflected in the experiment for PLA, which is made of homogeneous materials, the effect of porosity can be more straightforwardly related to Young's modulus. Generally, adding more porosity to the structure means introducing more voids, which act as stress concentrators and cause more significant disruption to the material's load-bearing structure. This situation reduces its ability to resist deformation. Based on the study by S. Lurie et al. (2018), the microstructure parameters can be porosity, shape and size of the pores, and the strength of the specimen reduces exponentially with the porosity[21]. Polymer structure with lower porosity is expected to retain much of its structural integrity and be capable of handling moderate compressive stresses. However, as porosity increases higher, the stiffness is greatly reduced, and the material becomes significantly less effective in resisting compression. The material is more prone to deformation, and the structure's ability to withstand compressive forces is further compromised and easily fractured.

Mathematically, the porous structure's bending due to the loss of stability can be explained using buckling phenomena, which could provide valuable insights from Equation (3). The Euler formula for critical buckling load can be related to this behavior, especially considering the aspects of deformation, energy absorption, and plastic deformation. Based on the previous study done by M. Sadeq Selat et al. (2018) under compression, the buckling load can be predicted based on the Euler buckling model, and the buckling load is dependent on the sample geometry [4]. In the study, the effect of grain and porosity was considered microstructure, which increases these microstructures, decreasing effective stiffness and increasing stress intensity. Meanwhile, Aamer Nazir et al. (2021) demonstrated the effect of the pore geometry design on critical buckling loads. The study found that a lower mass structure recorded a lower critical buckling load. As a homogeneous material with a simple shape, the moment of inertia was calculated using the geometry of the cross-section. However, when dealing with porous materials or irregular shapes, the relationship between the moment of inertia and the shape factor becomes more significant. The formula provides insights into the critical load where buckling-related bending occurs. Beyond this point, the plastic deformation described leads to irreversible changes in shape, which causes the structure to bend and the strut to slide to the side.

4.2 Effect of Porosity and Pore Shape

Pores interrupt the continuity by reducing the ability to resist axial compressive loads. As a result, the material's compressive strength decreases with increasing porosity. The impact of porosity on compression strength varies with the pore shape and size. For example, in metals, porosity is generally disadvantageous to compression strength as it limits the application of porous metal. In contrast, in this study, the controlled porosity of PLA alters its structure and polymer properties. It adds more value, such as energy absorption and pore, encouraging better heat dissipation.

Square pores tend to induce higher stress concentrations at their corners than circular pores. When a material is subjected to compression, the corners of square pores can act as stress concentrators, leading to localised stress concentrations. Square pores can introduce anisotropic behaviour in the material, meaning they may have different compressive strengths in different directions. Square pores with a higher aspect ratio (longer sides) may significantly reduce strength more than those with a lower aspect ratio.

Adding more porosity using 3D printing introduces unwanted voids within the printed layer, which softens the structure. Besides, higher porosity means a greater volume of voids or empty spaces within the structure. Introducing higher void content in a material has several implications for the porous polymer. One of the effects is that the presence of voids reduces the overall density of the material [22]. As a result, the material becomes less dense and, in turn, less bulk.

In some aspects, the unwanted void in the structure is managed as a defect of the 3D printing process, which must be removed once it is in the printed structure. However, even if the affected model undergoes the treatment process of sintering, the void is still there with the smaller size. Besides that, the printing strategy also affects the formation of the void, which is the attachment between the shell line of the outer side (mostly printed vertically 90 degrees) at a specific part of the sample with an adjacent printing line (print in 45 degrees) form two different contour lines also ponder as formation of the void in structure which not include as porosity. Besides that, in some cases, the void formation is also influenced by the material properties of the porous polymer. The study by K. S. Patel et al. (2023) mentioned that PLA is a strong and hard material. However, the 3D printing process leads to

higher void content in the printed structure [23]. The strength can be improved by introducing fibre to the material.

Microstructural changes could influence secondary stress softening in porous polymer structures, the rearrangement of polymer chains, or the collapse of specific pore structures under increasing compression [24, 25]. Understanding the specific causes would require more detailed analysis and investigation. Both primary and secondary stress softening are crucial for engineers and material scientists designing and utilising porous polymer structures. It informs decisions related to material selection, structural integrity, and performance in applications that involve compression or deformation.

5. Conclusion

The study highlights the significant impact of porosity and pore shape on the compressive strength of porous polymer structures. As porosity increases from 30% to 70%, a linear decrease in the maximum compression force for both square and circular pores is obtained. Higher porosity reduces load-bearing capacity, with circular pores initially showing greater strength. As the compression load applied increased, buckling occurred, leading to bending as the structure lost stability and stress reduction. Higher porosity consistently means lower compression strength. Circular pores have a stronger structure than square pores. Examining the collapse of the porous polymer structure under axial compression revealed significant differences between square and circular pores. Square pores collapsed more extensively, highlighting the role of curved walls in strengthening circular pores. Based on this study, the effect of the primary and secondary stress softening on the structural rupture is suggested to be explored. The phenomenon is particularly significant in structural applications where materials experience the applied load. In this study, for example, the porous polymer subjected to the compression load, the material experiences a reduction in stiffness and a change in the material's mechanical properties, primarily due to microstructural changes such as the breakdown of cross-links or the alignment of polymer chains. The result offered important details, helping to understand the connections between porosity, compression force, and the structure's strength. Besides, it emphasizes the critical influence of porosity and pore geometry on porous polymers' compressive strength and deformation behavior. It provides valuable insights for material design and optimization in various engineering applications.

Acknowledgement

No source of funding was used to complete this article.

Conflict of Interest

The author declares that there is no conflict of interest regarding the paper's publication.

Author Contribution

The author confirms sole responsibility for the following: study conception and design, data collection, analysis and interpretation of results, and manuscript preparation.

References

[1] K. K. Sadasivuni *et al.*, "A review on porous polymer composite materials for multifunctional electronic applications," *Polymer-Plastics Technology and Materials,* vol. 58, no. 12, pp. 1253-1294, 2019.

[2] S.-T. Schmitz-Hertzberg, R. Liese, C. Terjung, and F. F. Bier, "Towards a Smart Encapsulation System for Small-Sized Electronic Devices: A New Approach," *International Journal of Polymer Science,* vol. 2014, p. 713603, 2014/02/09 2014, doi: 10.1155/2014/713603.

[3] J. Parthasarathy, B. Starly, and S. Raman, "A design for the additive manufacture of functionally graded porous structures with tailored mechanical properties for biomedical applications," *Journal of Manufacturing Processes,* vol. 13, no. 2, pp. 160-170, 2011.

[4] M. S. Saleh, M. HamidVishkasougheh, H. Zbib, and R. Panat, "Polycrystalline micropillars by a novel 3-D printing method and their behavior under compressive loads," *Scripta Materialia,* vol. 149, pp. 144-149, 2018.

[5] C. Boursier Niutta, R. Ciardiello, and A. Tridello, "Experimental and numerical investigation of a lattice structure for energy absorption: application to the design of an automotive crash absorber," *Polymers,* vol. 14, no. 6, p. 1116, 2022.

[6] S. N. Yeole, P. Satyanarayana, K. Prakash, and P. Narendra, "Development of hydrophobic coating on 3D printed ABS samples and surface characterisation," *Journal of Mechanical Engineering and Sciences,* pp. 9791-9810, 2023.

[7] M. Y. Ab Aziz, K. M. Md Isa, M. A. f. Mohd Szali, M. Johar, and J. H. Mahmud, Muhamad Noor, "Fracture characteristics of PLA synthetic bone scaffolds with different specimen porosities," *Journal of Engineering Science and Technology,* vol. 18, no. 5, pp. 2493-2506, 2023.
[8] M. Y. M. S. Ab Aziz, Mohd Al fatihhi Abu Kasim, Haszeme, A. N. Rusli, and N. H. H. Noordin, Muhammad Nazif "Fracture mechanism analysis of bone scaffold under tensile load: The effect of porosity," *Journal of Engineering Science and Technology,* vol. 18, no. 5, pp. 2254-2268, 2023.
[9] S. A. Park *et al.*, "In Vivo Evaluation of 3D-Printed Polycaprolactone Scaffold Implantation Combined with β-TCP Powder for Alveolar Bone Augmentation in a Beagle Defect Model," *Materials,* vol. 11, no. 2, p. 238, 2018. [Online]. Available: https://www.mdpi.com/1996-1944/11/2/238.
[10] Y. Xue *et al.*, "Integration of electrospray and digital light processing for freeform patterning of porous microstructures," *Advanced Materials Technologies,* vol. 5, no. 11, p. 2000578, 2020.
[11] M. B. H. Othman, Z. Ahmad, and H. M. Akil, "Fabrication of nanoporous polyimide of low dielectric constant," in *2008 33rd IEEE/CPMT International Electronics Manufacturing Technology Conference (IEMT)*, 2008: IEEE, pp. 1-4.
[12] R. Kiran, A. Kumar, V. S. Chauhan, R. Kumar, and R. Vaish, "Finite element study on performance of piezoelectric bimorph cantilevers using porous/ceramic 0–3 polymer composites," *Journal of Electronic Materials,* vol. 47, pp. 233-241, 2018.
[13] K. Monkova, M. Vasina, M. Zaludek, P. P. Monka, and J. Tkac, "Mechanical Vibration Damping and Compression Properties of a Lattice Structure," *Materials,* vol. 14, no. 6, p. 1502, 2021. [Online]. Available: https://www.mdpi.com/1996-1944/14/6/1502.
[14] A. Nazir, M. Ali, and J.-Y. Jeng, "Investigation of Compression and Buckling Properties of a Novel Surface-Based Lattice Structure Manufactured Using Multi Jet Fusion Technology," *Materials,* vol. 14, no. 10, p. 2599, 2021. [Online]. Available: https://www.mdpi.com/1996-1944/14/10/2599.
[15] A. Goriely, R. Vandiver, and M. Destrade, "Nonlinear euler buckling," *Proceedings of the Royal Society A: Mathematical, Physical and Engineering Sciences,* vol. 464, no. 2099, pp. 3003-3019, 2008.
[16] B. Dorweiler, P. E. Baqué, R. Chaban, A. Ghazy, and O. Salem, "Quality control in 3D printing: accuracy analysis of 3D-printed models of patient-specific anatomy," *Materials,* vol. 14, no. 4, p. 1021, 2021.
[17] T. Hoskins, K. Dearn, and S. Kukureka, "Mechanical performance of PEEK produced by additive manufacturing," *Polymer testing,* vol. 70, pp. 511-519, 2018.
[18] J. R. C. Dizon, A. H. Espera, Q. Chen, and R. C. Advincula, "Mechanical characterisation of 3D-printed polymers," *Additive Manufacturing,* vol. 20, pp. 44-67, 2018/03/01/ 2018, doi: https://doi.org/10.1016/j.addma.2017.12.002.
[19] A. Field, *Discovering statistics using IBM SPSS statistics*. sage, 2013.
[20] E. Salje, J. Koppensteiner, W. Schranz, and E. Fritsch, "Elastic instabilities in dry, mesoporous minerals and their relevance to geological applications," *Mineralogical Magazine,* vol. 74, no. 2, pp. 341-350, 2010.
[21] S. Lurie, Y. Solyaev, L. Rabinskiy, P. Polyakov, and I. Sevostianov, "Mechanical behavior of porous Si 3 N 4 ceramics manufactured with 3D printing technology," *Journal of materials science,* vol. 53, pp. 4796-4805, 2018.
[22] P. Ferretti *et al.*, "Relationship between FDM 3D Printing Parameters Study: Parameter Optimisation for Lower Defects," *Polymers,* vol. 13, no. 13, p. 2190, 2021. [Online]. Available: https://www.mdpi.com/2073-4360/13/13/2190.
[23] K. S. Patel, D. B. Shah, S. J. Joshi, and K. M. Patel, "Developments in 3D printing of carbon fiber reinforced polymer containing recycled plastic waste: A review," *Cleaner Materials,* vol. 9, p. 100207, 2023/09/01/ 2023, doi: https://doi.org/10.1016/j.clema.2023.100207.
[24] L. C. Van Breemen, T. A. Engels, E. T. Klompen, D. J. Senden, and L. E. Govaert, "Rate‐ and temperature‐dependent strain softening in solid polymers," *Journal of Polymer Science Part B: Polymer Physics,* vol. 50, no. 24, pp. 1757-1771, 2012.
[25] K. Chen and K. S. Schweizer, "Theory of Yielding, Strain Softening, and Steady Plastic Flow in Polymer Glasses under Constant Strain Rate Deformation," *Macromolecules,* vol. 44, no. 10, pp. 3988-4000, 2011/05/24 2011, doi: 10.1021/ma200436w.